

# From Biomass to Polymers: Kinetic Analysis and Sustainable Synthesis of Lignin-Polycaprolactone Copolymers

Tim Langletz,<sup>[a, b]</sup> Medea Edinger,<sup>[a]</sup> Alexander Hoffmann,<sup>[a]</sup> and Sonja Herres-Pawlis<sup>\*,[a, b]</sup>

With 300 billion tons available in the biosphere, lignin is the second most abundant biopolymer on Earth. However, less than two percent is used for value-added applications. One potential application is the use of lignin as a building block for thermoplastics. The majority of plastics today are made from fossil-based feedstocks. Therefore, the use of lignin can counteract the increasingly scarce petroleum resources. A highly useful approach is the copolymerization with cyclic lactones such as caprolactone (CL) via ring-opening polymerization (ROP). The synthesis of lignin-polycaprolactone (PCL) copolymers can help to combine the beneficial properties of PCL and lignin to create potential new applications. In this work, lignin-PCL copolymers

are synthesized in a sustainable approach using the nontoxic, highly active, and robust zinc-based guanidine catalyst  $[Zn\{(R,R)\text{-DMEG}_2(1,2)\text{ch}_2\}_2]\text{OTf}_2 \cdot \text{THF}$ . Analyzing the reaction kinetics, it was found that the pseudo-first order reaction kinetics do not proceed with a uniform rate constant over the entire reaction. An acceleration occurs after the initial formation of PCL chains at the lignin core, with reaction rates depending on both the catalyst and lignin content. These new findings contribute to the mechanistic understanding behind lignin functionalization, highlighting the potential of such bio-based copolymers for a sustainable plastic use.

## 1. Introduction

Lignin is the second most abundant biopolymer on Earth after cellulose and is the main component of plant cell walls. Depending on the plant, the lignin content typically varies from 15% to 40% in wood and from 15% to 21% in straw species.<sup>[1,2]</sup> As a by-product of the pulp and paper industry, lignin is produced in large quantities, reaching almost 116 million tons in 2020, with an increasing trend.<sup>[3]</sup> There are approximately 300 billion tons of lignin available in the biosphere, increasing every year.<sup>[4]</sup> Currently, less than 2% is used for the production of value-added products, primarily for dispersants, adhesives, and surfactants, whereas 98% are burned for the generation of energy or treated as waste. In recent years, there has been a growing interest in lignin processing and researchers around the world are attempting to utilize lignin for other applications such as bioplastics, carbon fibers, fine chemicals, batteries, and

medical applications.<sup>[5–8]</sup> Due to its abundance and renewability, the utilization of lignin as a feedstock for the production of value-added products can help substitute fossil-based materials, such as plastics, fuels, or other chemicals, and thus contribute to a more sustainable chemical industry.<sup>[5]</sup> Furthermore, unlike some other biomass sources, the use of lignin as a feedstock does not compete with the food industry, making it even more attractive.<sup>[9]</sup> However, its heterogenous and nonuniform structure poses major challenges for valorization.<sup>[10]</sup>

Chemically, lignin consists of three phenylpropanoid units: coniferyl alcohol (G-type), sinapyl alcohol (S-type) and, to a lesser extent, *p*-coumaryl alcohol (H-type), which form a complex, three-dimensional (3D), and cross-linked network. The actual structure depends on several factors such as the type of plant and tissue, its age, environmental factors during plant growth, and the extraction process.<sup>[11]</sup> Two thirds of the bond types between the monomer units are ether linkages, the majority of which are alkyl aryl ether ( $\beta$ -O-4) bonds, whereas other major linkages include phenylcoumaran ( $\beta$ -5), pinosresinol ( $\beta$ - $\beta$ ), 1,2-diarylpropane ( $\beta$ -1), and biphenyl (5-5) bonds, among others.<sup>[12,13]</sup> Furthermore, lignin contains a variable proportion of aliphatic and aromatic hydroxyl moieties, which are excellent targets for functionalization.<sup>[14]</sup> Various strategies for the valorization of lignin are described in the literature. One approach is the synthesis of polymers from small molecules derived from lignin.

Gao et al. reported the synthesis of polymer networks based on magnolol, a phenolic compound derived from lignin. The magnolol was converted to an epoxy prepolymer and with the help of a borate ester-containing crosslinking agent, the polymer network was synthesized by a UV-induced thiol-ene click reaction. The resulting material exhibited good mechanical properties, which were largely retained even after up to three recycling cycles. In addition, the transparent material showed

[a] T. Langletz, M. Edinger, Dr. A. Hoffmann, Prof. Dr. S. Herres-Pawlis  
Institute of Inorganic Chemistry, RWTH Aachen University, Landoltweg 1a,  
Aachen 52074, Germany  
E-mail: [sonja.herres-pawlis@ac.rwth-aachen.de](mailto:sonja.herres-pawlis@ac.rwth-aachen.de)

[b] T. Langletz, Prof. Dr. S. Herres-Pawlis  
Bioeconomy Science Center (BioSC), Forschungszentrum Jülich GmbH, Jülich  
52425, Germany

Supporting information for this article is given via a link at the end of the document.

Supporting information for this article is available on the WWW under  
<https://doi.org/10.1002/cctc.202500589>

© 2025 The Author(s). ChemCatChem published by Wiley-VCH GmbH. This is an open access article under the terms of the [Creative Commons Attribution License](#), which permits use, distribution and reproduction in any medium, provided the original work is properly cited.

excellent self-healing properties, blocked UV radiation and had a thermal decomposition temperature of 300 °C, which is higher than conventional polyurethane networks.<sup>[15]</sup> Similarly, Gao et al. synthesized polyurethane thioether networks using eugenol as the initial material. First, eugenol was reacted with diisocyanates and subsequent crosslinking with a trithiol via a photoinduced thiol-ene click reaction yielded the desired polymeric networks. The resulting networks exhibited high mechanical performance, high thermal stability, intrinsic UV protection, and shape memory behavior.<sup>[16]</sup> Another approach for valorization of lignin is the direct functionalization. For example, lignin can be used in the synthesis of bio-based polyurethane foams as a substitute for petroleum-based polyols. The incorporation of lignin can provide several benefits, such as improved flame retardancy, thermal stability, UV resistance, and biodegradability, as well as lower product costs.<sup>[17,18]</sup> Moreover, Lee et al. demonstrated the synthesis of lignin-based polyesters through oxypropylation using propylene oxide, followed by sulfuric acid-catalyzed esterification with dicarboxylic acids, such as sebacic acid, or dicarboxy-terminated polybutadiene. The resulting polymers exhibited enhanced thermal properties compared with both the original lignin and the oxypropylated lignin.<sup>[19]</sup>

Additionally, lignin can be used for the synthesis of thermoplastic materials via copolymerization.<sup>[20]</sup> One approach is the ring-opening polymerization (ROP) of cyclic lactones, such as  $\epsilon$ -caprolactone (CL) or lactide (LA).<sup>[21,22]</sup> Usually, ROP is carried out in the presence of an alkoxide as co-initiator along with the catalyst. When lignin is used in the polymerization process, it can act as the co-initiator and the polymer chains grow from the hydroxyl moieties.<sup>[23]</sup> Polycaprolactone (PCL) is a biodegradable, semicrystalline, aliphatic polyester, which is used, among others, in packaging, tissue engineering, and drug delivery systems.<sup>[23–27]</sup> Due to its favorable properties such as mechanical strength, biocompatibility, biodegradability, ease of processability, and nontoxicity, PCL has been extensively researched.<sup>[23]</sup> Additionally, PCL is widely miscible with other polymers, and its monomer CL can be derived from renewable resources, primarily from sugar.<sup>[28]</sup> Lignin-polycaprolactone (PCL) copolymers can combine advantageous properties of both PCL and lignin, giving access to tailor-made bioplastics for specific and potentially new applications.<sup>[28–30]</sup>

As with many chemical reactions, the choice of catalyst is of crucial importance in the ROP of cyclic lactones. A wide range of different catalysts has been published, such as enzymes, organocatalysts, and metal-based catalysts including magnesium, calcium, tin, zinc, titanium, iron, and manganese.<sup>[23,31–42]</sup> Specifically for the grafting of CL onto lignin, the most prominent catalysts are tin-based compounds such as tin 2-ethylhexanoate or dibutyltin dilaurate.<sup>[28,30,43,44]</sup> These catalysts are effective, commercially available, and show high activity in the ROP of CL.<sup>[23]</sup> However, the main drawback is the cytotoxicity of tin compounds, which remain in the final polymer and may aggregate or pollute the environment after (bio)degradation.<sup>[45,46]</sup> To solve this, Chu et al. reported the successful synthesis of lignin-PCL copolymers using 1,5,7-triazabicyclo[4.4.0]dec-5-ene (TBD) as catalyst under solvent-free conditions after 24 h.<sup>[47]</sup> Abdollahi et al. showed the copolymer-

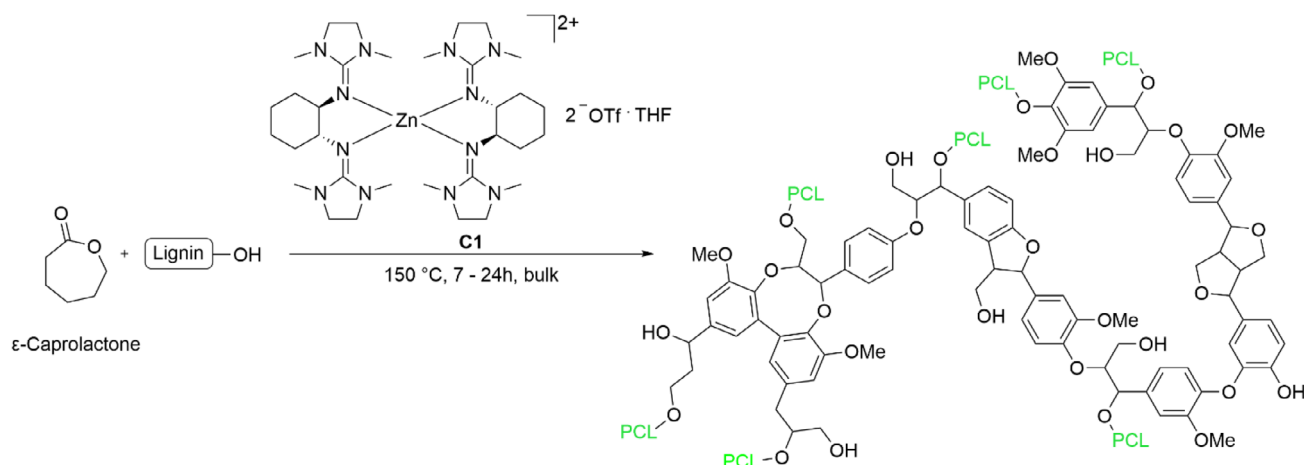
ization of lignin and CL in the presence of a nontoxic  $\text{ZnCl}_2$  catalyst. However, problems arose in this reaction. Trace amounts of HCl in the lignin, coming from the extraction process, combined with the catalyst, led to the partial formation of chlorine end groups and subsequent formation of water in the reaction system. This water can act as co-initiator during the ROP as well, leading to formation of PCL homopolymer during the copolymerization process.<sup>[48]</sup> This highlights the importance of finding alternative, nontoxic, efficient, and robust catalyst systems for the polymerization process under industrially relevant conditions.

In this work, we report an efficient route for the bulk copolymerization of CL with lignin using the highly active and nontoxic<sup>[49]</sup> zinc-based guanidine catalyst  $[\text{Zn}\{(\text{R},\text{R})\text{-DMEG}_2(1,2\text{ch})_2\}\text{OTf}_2 \cdot \text{THF}$  (**C1**). This catalyst has been previously reported for the synthesis of PLA under industrially relevant conditions,<sup>[39]</sup> as well as for the copolymerization of lignin and PLA<sup>[50]</sup> and alcoholysis of polyesters.<sup>[51]</sup> Due to its outstanding performance, **C1** was a well-suited candidate for the copolymerization of lignin and CL. Kinetic investigations were carried out to gain insights into the reaction mechanism for the first time in this chemistry.

## 2. Results and Discussion

Copolymerization reactions were carried out under industrially relevant conditions in the absence of any solvent at 150 °C with varying lignin and catalyst loadings using **C1** (Scheme 1). Thermogravimetric analysis (TGA) was carried out to confirm that lignin is stable under the reaction conditions and no significant degradation was observed (Figure S31). Reaction kinetics were investigated using  $^1\text{H}$  nuclear magnetic resonance (NMR) spectroscopy and the resulting polymers were analyzed via  $^1\text{H}$  NMR,  $^{31}\text{P}$  NMR spectroscopy, diffusion-ordered spectroscopy (DOSY) and size exclusion chromatography (SEC). By derivatization of lignin with 2-chloro-4,4,5,5-tetramethyl-1,3,2-dioxaphospholane (TMDP), the quantity of hydroxyl groups is accessible.<sup>[52]</sup> Since the initiation of the ROP occurs at the hydroxyl moieties and the chains grow from these groups, this is an important property of the lignin. To determine the molar mass of the lignin, acetylation was carried out prior to SEC analysis to increase the solubility in the mobile phase.<sup>[48]</sup> Table 1 summarizes the obtained results of the lignin characterization.

First, reactions with a lignin loading of 30 wt% were carried out to investigate the activity of the catalyst within the reaction system. A CL conversion of 90% was achieved after 7 h, which proved the activity and compatibility of **C1** toward the reaction system (Table 2, entry 3). DOSY NMR spectra of the corresponding copolymer showed a distinct diffusion coefficient, strongly supporting the formation of a chemically bonded lignin-PCL copolymer (Figures S19–S25), whereas a mixture of lignin and PCL shows two diffusion coefficients for the methoxy signals of lignin and PCL signals, respectively (Figure S26). SEC measurements showed a shift and broadening of the peak of the copolymers compared to pure lignin (Figure S27). This indicates that a copolymerization between lignin and CL has occurred to form a



**Scheme 1.** Reaction scheme of the copolymerization of lignin with  $\epsilon$ -caprolactone using  $[Zn\{(R,R)\text{-DMEG}_2(1,2)\text{ch}_2\}_2]\text{OTf}_2 \cdot \text{THF}$  (C1).

**Table 1.** Hydroxyl content and molar mass of the organosolv lignin used for copolymerization.

Aliphatic OH <sup>a)</sup> [mmol g <sup>-1</sup> ]	Aromatic OH <sup>a)</sup> [mmol g <sup>-1</sup> ]	Carboxylic OH <sup>a)</sup> [mmol g <sup>-1</sup> ]	Total OH <sup>a)</sup> [mmol g <sup>-1</sup> ]	$M_n^b)$ [g mol <sup>-1</sup> ]	$M_w^b)$ [g mol <sup>-1</sup> ]	$\bar{P}^b)$
1.71	4.18	0.11	6.00	1151	2365	2.1

<sup>a)</sup> Determined by <sup>31</sup>P NMR spectroscopy after phosphitylation with TMDP according to a literature procedure with cyclohexanol as internal standard.<sup>[52]</sup>  
<sup>b)</sup> Determined by SEC in THF using a conventional calibration with polystyrene standards. Molar masses given in polystyrene equivalents.

**Table 2.** Experimental data for the copolymerization of lignin and CL.

Entry	Lignin Loading (wt%)	CL/OH Ratio	Catalyst Loading <sup>a)</sup>	Conversion (%) <sup>b)</sup>	Time (h)	$DP_{n, \text{theo}}^c)$	$DP_{n, \text{exp}}^d)$
1	10	13.2	100:1	88	5.5	10	25
2	30	3.4	100:1	90	7	3	11
3	50	1.5	100:1	54 (92)	7 (24)	1	6
4	30	3.4	150:1	52 (96)	7 (24)	3	11
5	30	3.4	200:1	47 (94)	7 (24)	3	11
6	30	3.4	250:1	35 (95)	7 (24)	3	11
7 <sup>e)</sup>	30	3.4	100:1	75	7	3	7

<sup>a)</sup> Refers to the molar ratio of CL to catalyst.  
<sup>b)</sup> Determined by <sup>1</sup>H NMR spectroscopy.  
<sup>c)</sup>  $DP_{n, \text{theo}}$  calculated by conversion \*  $([\text{CL}]/([\text{OH}]_{\text{lignin}}))$ .  
<sup>d)</sup> Determined by end group integration of <sup>1</sup>H NMR spectra according to the literature.<sup>[30]</sup>  
<sup>e)</sup> TBD used as catalyst instead of C1.

multi-arm star-shaped polymer, a structure also reported in the literature.<sup>[29]</sup> Subsequently, lignin loadings were varied between 10 to 50 wt% to investigate how the reaction system is influenced by the lignin loading (Table 2, entries 1–3). Lowering the lignin loading and thus increasing the concentration of CL leads to a slightly faster reaction, whereas 88% conversion is reached after 5.5 h, compared to 54% after 7 h while using 50 wt%. This indicates different reactivities of the CL toward the ROP. This could be explained by the fact that CL is a rather nonpolar molecule that must first diffuse to the polar hydroxyl groups of lignin in the reaction mixture for ROP to take place. It might be that this step determines the rate of the reaction and that the ring opening of CL is facilitated if a previous monomer has already been

ring-opened and reacted with the hydroxyl group of the lignin. This would cause the reactive centers to lose polarity, facilitating the diffusion of CL and ultimately accelerating the reaction. As the total amount of lignin and therefore the total amount of functionalizable hydroxyl groups is lower at low lignin contents, the polymer chains grow faster to higher chain lengths, which has an accelerating effect on the reaction rate. The effect of catalyst concentration was subsequently investigated by varying the catalyst loading between 100:1 and 250:1 with respect to CL (Table 2, entries 2 and 4–7). Conversions after 7 h decreased with decreasing catalyst loading, which is the expected trend since the catalyst is required for the activation of CL. Since the conversions directly influence the chain lengths and thus the

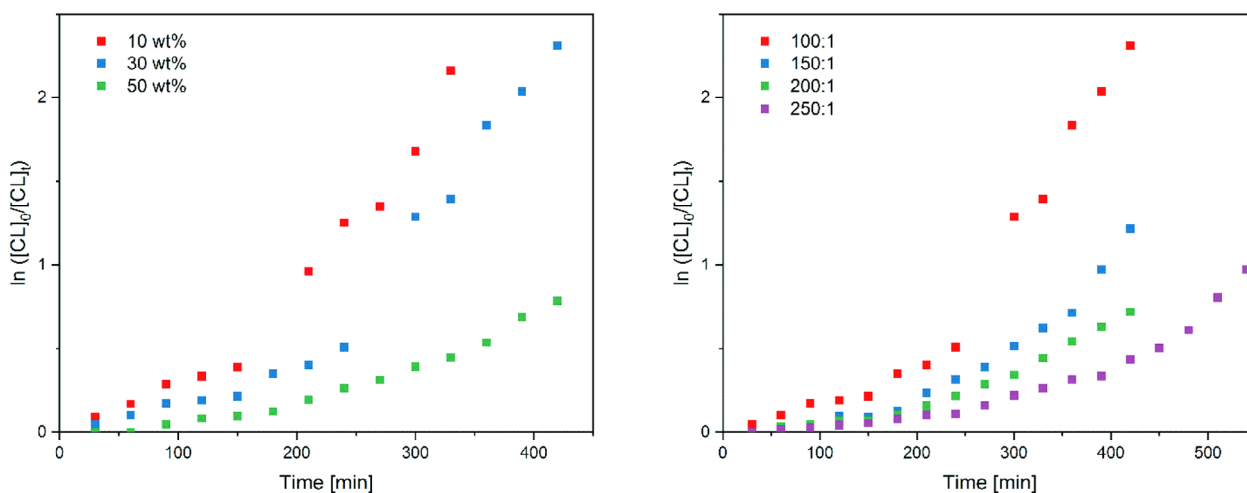


**Figure 1.** Semi-logarithmic plots for copolymerization reactions ( $T = 150\text{ }^{\circ}\text{C}$  and  $t = 5.5\text{--}9\text{ h}$ ) with varying lignin loadings and a catalyst loading of 100:1 (left) and a fixed lignin loading of 30 wt% and varying catalyst loadings (right).

molar mass of the copolymer, the reaction times were increased to 24 h to ensure high conversions for subsequent analysis. The PCL chain lengths and thus the degree of polymerization ( $DP$ ) vary in the sense that shorter chains are formed with increasing lignin content as the total number of functionalizable hydroxyl groups increases and thus the total number of PCL chains in the copolymers increases. A comparison of the experimentally determined degree of polymerization ( $DP_{n, \text{exp}}$ ) shows that these are higher than theoretically calculated degree of polymerization ( $DP_{n, \text{theo}}$ ), suggesting incomplete functionalization at the lignin core. The relative difference between the two  $DP$ s gets more pronounced with increasing lignin loading, indicating that lignin is higher functionalized in copolymers with lower lignin loading (Table 2, entries 1–3). This is also confirmed by  $^{31}\text{P}$  NMR analysis of the derivatized polymers, which showed that copolymers with higher lignin contents have more free hydroxyl groups. In addition, it can be observed that the aliphatic hydroxyl groups are preferentially functionalized, which is consistent with findings from literature.<sup>[53]</sup> At lignin loadings of 10 and 30 wt%, the aliphatic hydroxyl groups are almost completely functionalized, whereas at 50 wt% lignin some of the aliphatic hydroxyl groups remain unfunctionalized (Table S1). Varying the catalyst concentration does not affect the PCL chain lengths and therefore does not affect the  $DP$  (Table 2, entries 4–6). Furthermore, TBD was tested as catalyst for copolymerization to allow direct comparison of the catalysts under the same reaction conditions (Table 2, entry 7). A lower conversion of 75% is achieved after a reaction time of 7 h, which explains that the observed  $DP_{n, \text{exp}}$  of this copolymer is only 7 instead of 11 compared to the entry for the copolymerization with **C1** (Table 2, entries 2 and 7). A comparison of the functionalization of the lignin core of these two copolymers using  $^{31}\text{P}$  NMR spectroscopy after derivatization shows similar functionalization of hydroxyl groups for both catalysts and suggests that the functionalization of hydroxyl groups is independent of the choice of catalyst.

To gain a better understanding of the reaction progress of the copolymerization, a kinetic analysis of the reaction was per-

formed (Figure 1). During the reaction, aliquots of the reaction mixture were taken and the conversion was determined by  $^1\text{H}$  NMR spectroscopy. The conversion  $X$  at any time  $t$  can be calculated from the signals of the repeating units of the PCL  $i_{\text{PCL}}$  chains ( $\delta_{\text{1H, DMSO}} = 2.27\text{ ppm}$ ) and the unreacted CL  $i_{\text{CL}}$  ( $\delta_{\text{1H, DMSO}} = 2.59\text{ ppm}$ ) (Figure S10).

Generally, the reaction kinetics of ring-opening polymerizations of cyclic lactones, such as CL or LA, are pseudo-first order and linear over most of the reaction course.<sup>[39,41,42,54–58]</sup> Linear kinetics were also observed for the copolymerization of lignin with lactide.<sup>[50]</sup> Here, the kinetics show a linear behavior, but the slopes of the linear plots appear to change during the reaction. Initially, the reaction proceeds more slowly until the reaction accelerates after about 3 h. For lignin contents of 10 and 30 wt%, the CL conversion of the reaction corresponds to about 25% to 30% at this point. This threshold is likely caused by the growing chain of the polymer, confirming the previously discussed hypothesis that the ring-opening of CL is facilitated when ROP occurs at the end of a growing PCL chain rather than directly at a hydroxyl group of the lignin core. A linear behavior can also be observed for the subsequent course of the reaction, but with a greater slope, indicating a higher reaction rate. The acceleration can also be seen for the polymer with a high lignin content of 50 wt%, but is less pronounced because the higher hydroxyl group content in the reaction mixture results in the formation of overall shorter PCL chains (Figure 1, left). This trend is also observed when the catalyst concentration in the reaction system is reduced. In addition, polymerizations are slower overall, proving that the catalyst is essential for the reaction to proceed (Figure 1, right). Additionally,  $^{31}\text{P}$  NMR spectroscopy was used to investigate the degree of functionalization of the lignin core as a function of conversion in derivatized copolymer samples with 30 wt% lignin (Figure S33). Only a few hydroxyl groups were found to be functionalized at the beginning of the reaction. Most of the hydroxyl groups were functionalized at conversions between 35% and 60%. Above 60%, hardly any additional hydroxyl groups are functionalized, and only chain-extending ring openings of



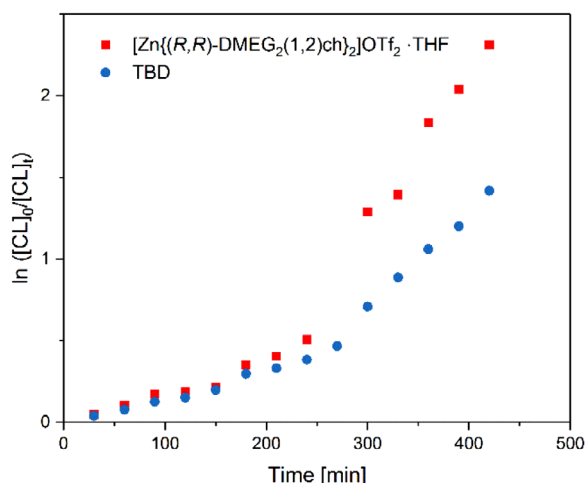


Figure 2. Comparison of the semi-logarithmic plots of TBD and C1 at 30 wt% lignin and a catalyst loading of 100:1.

the caprolactone occur. This phenomenon also affects the rate of the reaction and confirms the previously observed behavior of an induction phase of copolymerization. With a larger number of initial chains, the reaction accelerates further because several chains can polymerize simultaneously. Furthermore, the molecular weight of the growing PCL chain segments was examined throughout the reaction period. The results showed that the molecular weight increased linearly over the reaction period. Therefore, it can be concluded that this is a controlled copolymerization process in which chain-shortening transesterification reactions do not occur (Figure S32).

A comparison of the reaction kinetics of C1 and TBD at a fixed lignin loading of 30 wt% and a catalyst loading of 100:1 showed that the untypical course of the reaction kinetics also occurs with TBD as polymerization catalyst and can therefore most likely be observed independently of the catalyst (Figure 2). Furthermore, when comparing the reaction kinetics, it becomes clear that using C1 causes the copolymerization to proceed faster. This demonstrates the potential of  $[\text{Zn}\{(R,R)\text{-DMEG}_2(1,2)\text{ch}_2\}_2]\text{OTf}_2 \cdot \text{THF}$  as a nontoxic, highly active, and robust catalyst for the synthesis of lignin-PCL copolymers.

### 3. Conclusion

In this work, we presented a sustainable and efficient approach to synthesize lignin-PCL copolymers using a robust, nontoxic, and highly active zinc-guanidine catalyst  $[\text{Zn}\{(R,R)\text{-DMEG}_2(1,2)\text{ch}_2\}_2]\text{OTf}_2 \cdot \text{THF}$  via ring-opening polymerization. PCL chains are grafted onto the lignin directly in the melt without the use of additional solvents. Copolymers with different lignin contents and different catalyst loadings were successfully prepared, with DOSY NMR and SEC data showing a chemical linkage between lignin and PCL. Furthermore, kinetic studies for lignin-PCL copolymerization reactions were performed for the first time. Typically, the ROP of cyclic lactones follows linear pseudo-first order kinetics with constant reaction rates over the entire course of the reaction. In the case of lignin and CL

copolymerization, an acceleration of the reaction was observed, leading to an increasing reaction rate constant. The time at which the reaction is accelerated can be correlated with the conversion and therefore with the chain length of PCL segments. This is particularly noticeable at lower lignin loadings, as longer PCL chains are formed in a shorter period of time. For higher lignin loadings this is not as pronounced, because higher lignin loadings lead to the formation of shorter PCL chain segments overall, since the concentration of hydroxyl groups, which act as reactive centers during the ROP, is higher. In addition, the reaction kinetics of the catalyst were compared with the well-known organocatalyst TBD, with the reaction proceeding in a faster manner when using  $[\text{Zn}\{(R,R)\text{-DMEG}_2(1,2)\text{ch}_2\}_2]\text{OTf}_2 \cdot \text{THF}$  as catalyst.  $^{31}\text{P}$  NMR analysis after derivatization of the copolymers showed an incomplete functionalization at the lignin core, whereas more hydroxyl groups are functionalized at lower lignin loadings. In this case, the functionalization of the lignin was not affected by the choice of catalyst. These results contribute to the understanding of reaction mechanisms of lignin functionalization and to the development of alternative bio-based plastics to transition the plastic industry away from fossil-based feedstocks.

## 4. Experimental Section

### 4.1. Materials and Methods

All reactions were carried out under nitrogen atmosphere (99.999%), dried by  $\text{P}_4\text{O}_{10}$  using standard Schlenk techniques. Chemicals used within this work were purchased from Merck KGaA, Acros Organics, Th. Geyer GmbH & Co. KG, TCI Deutschland GmbH, abcr GmbH, and VWR Deutschland GmbH. Solvents were purchased in technical purity and distilled prior to use if needed.  $\epsilon$ -Caprolactone was distilled over  $\text{CaH}_2$  and stored under nitrogen prior to use. TMDP<sup>[59]</sup> and  $[\text{Zn}\{(R,R)\text{-DMEG}_2(1,2)\text{ch}_2\}_2]\text{OTf}_2 \cdot \text{THF}$ <sup>[39]</sup> were synthesized according to literature procedures. Organosolv lignin was kindly donated from Fraunhofer CPB Leuna and dried in a vacuum oven at 0.2 mbar for 24 h at 40 °C.

Nuclear magnetic resonance (NMR) spectra were recorded at 25 °C on a Bruker Avance III DH 400 or Bruker Avance II 400 nuclear magnetic resonance spectrometer operating at 400 MHz for  $^1\text{H}$  and 162 MHz for  $^{31}\text{P}$  spectra. Chemical shifts are given relative to resonances from the deuterated solvents ( $\text{DMSO}$ :  $\delta(^1\text{H}) = 2.50$  ppm,  $\text{CDCl}_3$ :  $\delta(^1\text{H}) = 7.26$  ppm).  $^{31}\text{P}$  Spectra were obtained as described in literature<sup>[52]</sup> and referenced to 132.2 ppm, which is the reaction product of TMDP and residual water. DOSY NMR measurements were carried out using  $^1\text{H}$  NMR standard processing applied on pseudo-2D datasets ( $\text{si} = 8$  k,  $\text{lb} = 0.3$ ,  $\text{xf}_2$ ,  $\text{abs}_2$ ). For the Bruker Avance III HD 400 the software Topspin (Version 3.5 pl 7) from Bruker and for the Bruker Avance II 400 the software TopSpin (Version 2.1) from Bruker were used for data acquisition. For visualization and examination of NMR spectra, the software MestReNova (Version 14.2.3–29241) from Mestrelab research was used.

The molecular weight of lignin-PCL copolymers was determined by size exclusion chromatography on a Viscotek GPCmax VE-2001 with a flow rate of  $1 \text{ mL min}^{-1}$  at 25 °C with THF as mobile phase. The system was equipped with two Malvern Viscotek T columns (porous styrene divinylbenzene copolymer) with a maximum pore size of 500 and 5000 Å, a HPLC pump, a refractive index detector (VE-3580), and a viscometer (Viscotek 270 Dual detector). For data acquisition, the software Omniseac 5.12 was used. The results were

evaluated using a conventional calibration using polystyrene standards. The respective molecular weights are given in polystyrene equivalents.

Thermogravimetric analysis of lignin and lignin-PCL copolymers were conducted on NETZSCH STA 449 F5 Jupiter. The samples were heated at a rate of 5 K per minute from 25 °C to 800 °C in a nitrogen atmosphere.

#### 4.2. General Procedure for the Synthesis of Lignin-PCL Copolymers

In a nitrogen filled glovebox, lignin and the catalyst were weighed into a flask and the appropriate amount of  $\epsilon$ -caprolactone was added. The flask was taken out of the glovebox and equipped with an overhead stirrer. The reaction mixture was heated to 150 °C and stirred at 150 rpm. For the kinetic investigations, aliquots were taken after specific time intervals, dissolved in deuterated dimethyl sulfoxide and the  $\epsilon$ -caprolactone conversion was determined by  $^1\text{H}$  NMR spectroscopy. After achieving sufficient conversion, the reaction mixture was cooled under running tap water. The mixture was dissolved in as little DCM as possible (10–20 mL) and precipitated in diethyl ether at 0 °C. The polymer was washed with cold methanol (25 mL) and dried at 0.2 mbar at 50 °C for 24 h. Lignin-PCL copolymers were obtained as darkish-brown solid.

#### 4.3. General Procedure for the Phosphitylation of Lignin-PCL Copolymers and Lignin

The phosphitylation experiments were conducted based on a modified literature procedure.<sup>[52]</sup> A mixture of pyridine and deuterated chloroform (1.6/1; v/v) was prepared and stored over molecular sieves 3 Å. A cyclohexanol solution (10 mg mL<sup>-1</sup>) and a solution of chromium(III) acetylacetonate (5 mg mL<sup>-1</sup>) was prepared from the pyridine/chloroform solution. Lignin (30 mg) or lignin-PCL copolymers (30 mg), respectively, were dissolved in the pyridine/chloroform solution (0.5 mL) and the chromium(III) acetylacetonate (50  $\mu\text{L}$ ), cyclohexanol solution (50  $\mu\text{L}$ ), as well as TMDP (75  $\mu\text{L}$ ) were added. The mixture was allowed to stir for 1 h for the lignin and for 24 h for the copolymers to ensure quantitative functionalization prior to  $^{31}\text{P}$  NMR spectroscopic analysis.

#### 4.4. General Procedure for the Acetylation of Lignin

Acetylation was carried out according to a modified literature procedure.<sup>[60]</sup> Lignin (1 g, c(OH) = 6.00 mmol g<sup>-1</sup>) was weighed into an oven-dried flask. Pyridine (5 mL) and acetic anhydride (5 mL, 52.9 mmol, 8.9 eq. with respect to the hydroxyl groups of lignin) were added and the mixture was stirred for 24 h at 20 °C. The crude reaction mixture was precipitated from a diluted HCl solution (250 mL, 0.1 M). The resulting precipitate was washed several times with deionized water to neutral pH. Finally, the product was dried at 0.2 mbar at 50 °C for 24 h.

### Acknowledgements

The authors acknowledge the financial support of the Bioeconomy Science Center as part of the project LignoTex. The scientific activities of the Bioeconomy Science Center were financially supported by the Ministry of Innovation, Science and Research within the framework of the NRW Strategieprojekt BioSC (no. 313/323-400-002 13). The authors thank Fraunhofer CPB Leuna

for organosolv lignin donations. And the authors also thank Noah Avraham-Radermacher from the Institute of Technical and Macromolecular Chemistry of the RWTH Aachen University for TGA measurements.

Open access funding enabled and organized by Projekt DEAL.

### Conflict of Interests

The authors declare no conflicts of interest.

### Data Availability Statement

NMR spectroscopic data and SEC data for the synthesis of lignin-polycaprolactone copolymers were deposited. These data were deposited as original data in the repository RADAR4Chem by FIZ Karlsruhe–Leibniz-Institut für Informationsinfrastruktur and are published under an Open Access model (CC BY-NC-SA 4.0 Attribution-NonCommercial-ShareAlike; <https://www.radar-service.eu/radar/en/dataset/h75gdvfp2xbwyejz>).

**Keywords:** Catalysis · Copolymerization · Renewable resources · Ring-opening polymerization

- [1] A. Tribot, G. Amer, M. Abdou Alio, H. de Baynast, C. Delattre, A. Pons, J.-D. Mathias, J.-M. Callois, C. Vial, P. Michaud, C.-G. Dussap, *Eur. Polym. J.* **2019**, *112*, 228–240.
- [2] S. H. Ghaffar, M. Fan, *Int. J. Adhes. Adhes.* **2014**, *48*, 92–101.
- [3] R. Nadányi, G. Zinovyev, M. Majerčík, M. Stosel, M. Jablonský, A. Ház, *Forests* **2024**, *15*, 1028.
- [4] J. Fernández-Rodríguez, X. Erdocia, C. Sánchez, M. González Alriols, J. Labidi, *J. Ener. Chem.* **2017**, *26*, 622–631.
- [5] D. S. Bajwa, G. Pourhashem, A. H. Ullah, S. G. Bajwa, *Ind. Crops Prod.* **2019**, *139*, 111526.
- [6] C. Wang, S. S. Kelley, R. A. Venditti, *ChemSusChem* **2016**, *9*, 770–783.
- [7] O. Yu, K. H. Kim, *Appl. Sci.* **2020**, *10*, 4626.
- [8] M. Norgren, H. Edlund, *Curr. Opin. Colloid Interface Sci.* **2014**, *19*, 409–416.
- [9] F. Cherubini, *Ener. Convers. Manage.* **2010**, *51*, 1412–1421.
- [10] M. Ullah, P. Liu, S. Xie, S. Sun, *Molecules* **2022**, *27*, 6055.
- [11] L. Schoofs, B. Thiele, J. Tonn, T. Langlet, S. Herres-Pawlis, A. Jupke, P. M. Grande, H. Klose, *Ener. Fuels* **2024**, *38*, 4192–4202.
- [12] L. A. Zevallos Torres, A. Lorenci Woiciechowski, V. O. de Andrade Tanobe, S. G. Karp, L. C. Guimarães Lorenci, C. Faulds, C. R. Soccol, *J. Cleaner Prod.* **2020**, *263*, 121499.
- [13] G. Gellerstedt, *Ind. Crops Prod.* **2015**, *77*, 845–854.
- [14] N.-E. E. Mansouri, J. Salvadó, *Ind. Crops Prod.* **2006**, *24*, 8–16.
- [15] D. Zhang, Y. Zhai, D. Zhang, L. Gao, *ACS Appl. Polym. Mater* **2024**, *6*, 9922–9931.
- [16] Y. Zhai, D. Zhang, L. Gao, *Biomacromolecules* **2024**, *25*, 5949–5958.
- [17] C. Xu, F. Ferdosian, in *Conversion of Lignin into Bio-Based Chemicals and Materials* (Eds.: C. Xu, F. Ferdosian), Springer Berlin Heidelberg, Berlin, Heidelberg, **2017**, 133.
- [18] H. Li, Y. Liang, P. Li, C. He, *J. Bioresour. Bioprod.* **2020**, *5*, 163–179.
- [19] Y. Lee, C.-H. Park, E. Y. Lee, *J. Wood Chem. Technol.* **2017**, *37*, 334–342.
- [20] M. Parit, Z. Jiang, *Int. J. Biol. Macromol.* **2020**, *165*, 3180–3197.
- [21] S. Kim, H. Chung, *Green Chem.* **2024**, *26*, 10774–10803.
- [22] A. P. Dove, *Chem. Commun.* **2008**, 6446–6470.
- [23] M. Labet, W. Thielemans, *Chem. Soc. Rev.* **2009**, *38*, 3484–3504.
- [24] E. H. Backes, S. V. Harb, C. A. G. Beatrice, K. M. B. Shimomura, F. R. Passador, L. C. Costa, L. A. Pessan, *J. Biomed. Mater. Res., Part B* **2022**, *110*, 1479–1503.
- [25] P. Mandal, R. Shunmugam, *J. Macromol. Sci., Part A: Pure Appl. Chem.* **2020**, *58*, 111–129.

- [26] M. Á. Corres, Á. Mayor, A. Sangroniz, J. del Río, M. Iriarte, A. Etxeberria, *Eur. Polym. J.* **2020**, *135*, 109869.
- [27] Y. Ikada, H. Tsuji, *Macromol. Rapid Commun.* **2000**, *21*, 117–132.
- [28] M. Li, Y. Pu, F. Chen, A. J. Ragauskas, *N. Biotechnol.* **2021**, *60*, 189–199.
- [29] J. Tian, Y. Yang, J. Song, *Int. J. Biol. Macromol.* **2019**, *141*, 919–926.
- [30] I. K. Park, H. Sun, S. H. Kim, Y. Kim, G. E. Kim, Y. Lee, T. Kim, H. R. Choi, J. Suhr, J. D. Nam, *Sci. Rep.* **2019**, *9*, 7033.
- [31] L. F. Sánchez-Barba, A. Garcés, M. Fajardo, C. Alonso-Moreno, J. Fernández-Baeza, A. Otero, A. Antiñolo, J. Tejeda, A. Lara-Sánchez, M. I. López-Solera, *Organometallics* **2007**, *26*, 6403–6411.
- [32] B. T. Ko, C. C. Lin, *J. Am. Chem. Soc.* **2001**, *123*, 7973–7977.
- [33] L. Piao, M. Deng, X. Chen, L. Jiang, X. Jing, *Polymer* **2003**, *44*, 2331–2336.
- [34] Archana Bhaw-Luximon, Dhanjay Jhurry, Shaheen Motala-Timol, Yemanlall Lochee, *Macromol. Symp.* **2006**, *231*, 60–68.
- [35] R. H. Platel, L. M. Hodgson, C. K. Williams, *Polym. Rev.* **2008**, *48*, 11–63.
- [36] H. Dong, H.-d. Wang, S.-g. Cao, J.-c. Shen, *Biotechnol. Lett.* **1998**, *20*, 905–908.
- [37] A. Mahapatro, A. Kumar, R. A. Gross, *Biomacromolecules* **2004**, *5*, 62–68.
- [38] L. Mezzasalma, J. de Winter, D. Taton, O. Coulembier, *Green Chem.* **2018**, *20*, 5385–5396.
- [39] Alina Hermann, Stephen Hill, Angela Metz, Joshua Heck, Alexander Hoffmann, Laura Hartmann, Sonja Herres-Pawlis, *Angew. Chem., Int. Ed. Engl.* **2020**, *59*, 21778–21784.
- [40] Ruth D. Rittinghaus, Johannes Zenner, Andrij Pich, Moshe Kol, Sonja Herres-Pawlis, *Angew. Chem. Int. Ed.* **2022**, *61*, e202112853.
- [41] Martin Fuchs, Pascal M. Schäfer, Wolf Wagner, Ian Krumm, Marcel Walbeck, Regina Dietrich, Alexander Hoffmann, Sonja Herres-Pawlis, *ChemSusChem* **2023**, *16*, e202300192.
- [42] C. Conrads, L. Burkart, S. Soerensen, S. Noichl, Y. Kara, J. Heck, A. Hoffmann, S. Herres-Pawlis, *Catal. Sci. Technol.* **2023**, *13*, 6006–6021.
- [43] W. de Oliveira, W. G. Glasser, *Macromolecules* **1994**, *27*, 5–11.
- [44] S. H. Kim, K. Choi, H. R. Choi, T. Kim, J. Suhr, K. J. Kim, H. J. Choi, J. D. Nam, *ACS Omega* **2019**, *4*, 10036–10043.
- [45] S. Jacobsen, H. G. Fritz, P. Degée, P. Dubois, R. Jérôme, *Polym. Eng. Sci.* **2004**, *39*, 1311–1319.
- [46] H. R. Kricheldorf, *Chemosphere* **2001**, *43*, 49–54.
- [47] X. Liu, E. Zong, J. Jiang, S. Fu, J. Wang, B. Xu, W. Li, X. Lin, Y. Xu, C. Wang, F. Chu, *Int. J. Biol. Macromol.* **2015**, *81*, 521–529.
- [48] M. Abdollahi, R. Bairami Habashi, M. Mohsenpour, *Ind. Crops Prod.* **2019**, *130*, 547–557.
- [49] C. Lackmann, J. Brendt, T. B. Seiler, A. Hermann, A. Metz, P. M. Schäfer, S. Herres-Pawlis, H. Hollert, *J. Hazard. Mater.* **2021**, *416*, 125889.
- [50] T. Langlet, P. M. Grande, J. Viell, D. Wolters, J. Tonn, H. Klose, S. G. Schriever, A. Hoffmann, A. Jupke, T. Gries, S. Herres-Pawlis, *Adv. Energy Sustainability Res.* **2023**, *5*, 2300187.
- [51] Tabea Becker, A. Hermann, Nazik Saritas, Alexander Hoffmann, Sonja Herres-Pawlis, *ChemSusChem* **2024**, *17*, e202400933.
- [52] A. Granata, D. S. Argyropoulos, *J. Agric. Food Chem.* **2002**, *43*, 1538–1544.
- [53] M. C. Najjarro, M. Nikolic, J. Iruthayaraj, I. Johannsen, *ACS Appl. Polym. Mater.* **2020**, *2*, 5767–5778.
- [54] Alina Hermann, Tabea Becker, Martin A. Schäfer, Alexander Hoffmann, Sonja Herres-Pawlis, *ChemSusChem* **2022**, *15*, e202201075.
- [55] R. D. Rittinghaus, P. M. Schäfer, P. Albrecht, C. Conrads, A. Hoffmann, A. N. Ksiazkiewicz, O. Bienemann, A. Pich, S. Herres-Pawlis, *ChemSusChem* **2019**, *12*, 2161–2165.
- [56] C. Lv, R. Yang, G. Xu, L. Zhou, Q. Wang, *Eur. Polym. J.* **2020**, *133*, 109792.
- [57] Y. Yu, G. Storti, M. Morbidelli, *Ind. Eng. Chem. Res.* **2011**, *50*, 7927–7940.
- [58] R. Mazarro, I. Gracia, J. F. Rodríguez, G. Storti, M. Morbidelli, *Polym. Int.* **2011**, *61*, 265–273.
- [59] P. Dais, A. Spyros, S. Christophoridou, E. Hatzakis, G. Fragaki, A. Agiomyrgianaki, E. Salivaras, G. Siragakis, D. Daskalaki, M. Tasioula-Margari, M. Brenes, *J. Agric. Food Chem.* **2007**, *55*, 577–584.
- [60] P. Buono, A. Duval, P. Verge, L. Averous, Y. Habibi, *ACS Sustain. Chem. Eng.* **2016**, *4*, 5212–5222.

Manuscript received: March 30, 2025

Revised manuscript received: June 2, 2025

Accepted manuscript online: June 3, 2025

Version of record online: ■■, ■■